

Supporting Information

Workfunction, a new viewpoint to understand the electrolyte/electrode interface reaction

Yurui Gao, Zhaoxiang Wang*, and Liquan Chen

Key Laboratory for Renewable Energy, Beijing Key Laboratory for New Energy Materials and Devices, Beijing National Laboratory for Condensed Matter Physics, Institute of Physics, Chinese Academy of Sciences, P. O. Box 603, Beijing 100190, China.

Email: zxwang@iphy.ac.cn, Tel & Fax: +86-10-82649050.

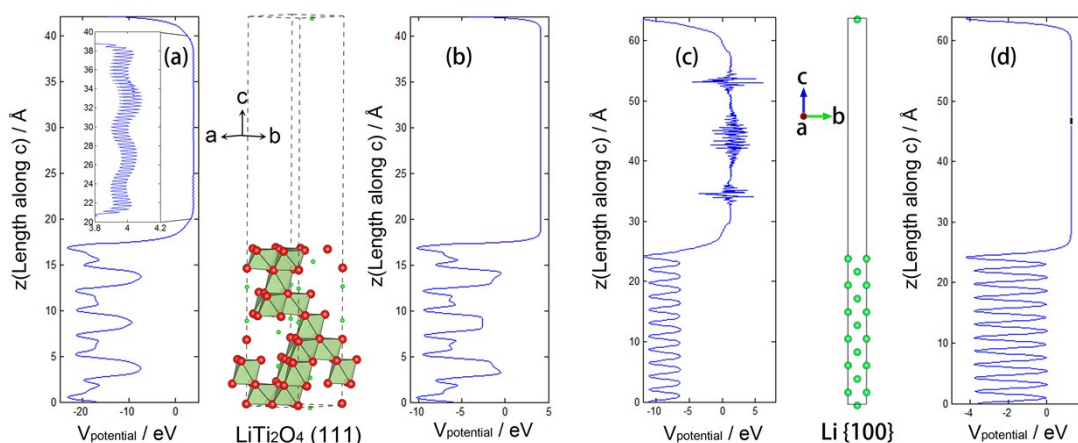


Fig. S1 Planar average of (a, c) the entire local potential energy and (b, d) the electrostatic potential energies along *c* of the LiTi₂O₄(111) surface model and the Li{100} surface, respectively. The insert of (a) is the enlargement of the entire local potential energy from 20 to 40 Å along *c* direction.

Fig. S1 shows that the entire local potential oscillates a little for the LiTi₂O₄(111) surface but strongly for the Li{100} surface when the exchange correlation part is considered. The average workfunction of the Li surfaces is used as the reference to locate the LUMO and HOMO of the electrolyte to be compared with the chemical potentials of the LiTi₂O₄ surfaces in this paper. Since the entire local potentials of Li surfaces oscillate strongly, only the electrostatic potentials are used in all the calculations to evaluate the workfunction for the sake of consistency. The difference caused by the exchange correlation part of the LiTi₂O₄ surfaces is ~ -0.1 eV and may be largely offset by the exchange correlation part of Li surfaces at comparison in Fig. 4 and therefore can be ignored.

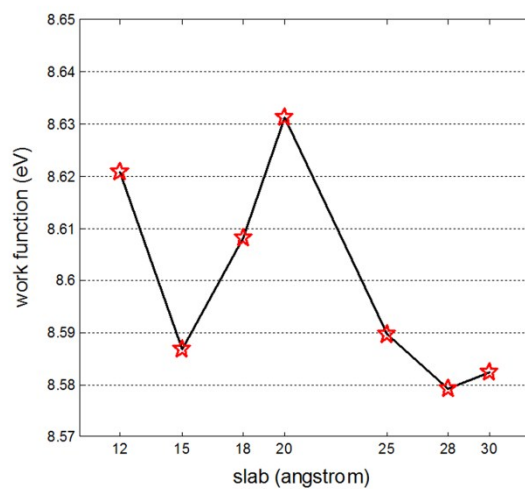


Fig. S2 The vacuum slab test for work function indicating that the workfunction gets convergent when the thickness of the vacuum slab is 25Å (though without U calibration for Ti-3d electrons, the result is applicable.).

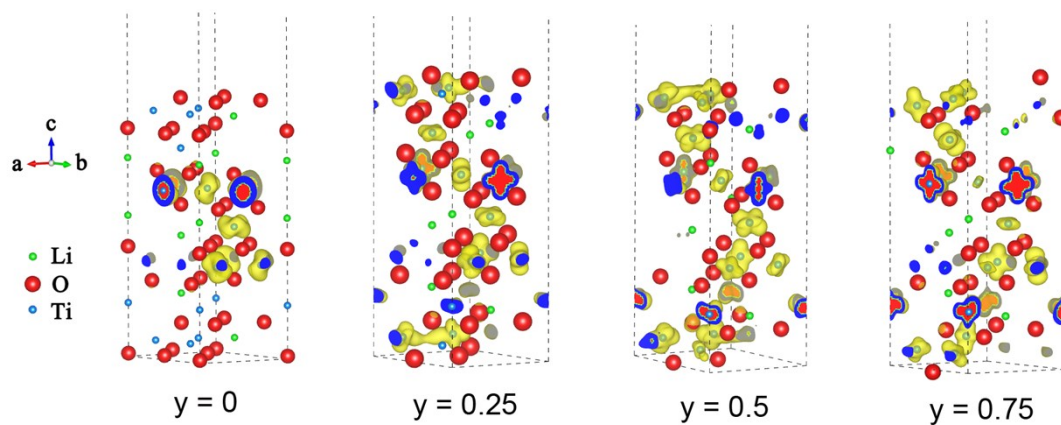


Fig. S3 Real-space distribution of the charge close to the Fermi level (from -1 to 0 eV) of LiTi_2O_4 with different coverages (y) of O vacancies on the (111) surface. All the energies refer to the Fermi level.

Table S1. Workfunction and atomic population, obtained by Bader analysis, of Ti on the Li-rich LiTi_2O_4 (111) surface with different Li-rich types.

Li-rich types	16c-m; 8a-n (to 16c)	16c-m and 16c-n; 8a-n (to 16c)
ϕ / eV	3.41	3.21
μ / eV	-0.75	-0.33
Φ / eV	4.16	3.54
Population: Ti1	1.364	1.701
Ti2	1.360	1.383
Ti3	1.361	1.373
$\text{Ti}^{3+}(1.66)$ contained in the bulk		

Note: Ti1, Ti2 and Ti3 are three Ti atoms on the surface.

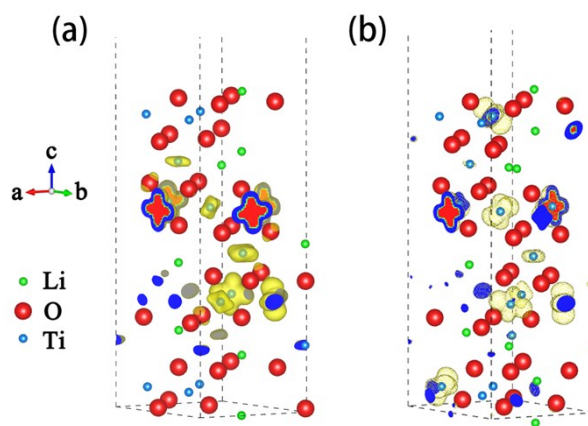


Fig. S4. Real-space distribution of the charge close to the Fermi level (from -1 to 0 eV) of LiTi_2O_4 with different Li-rich states on the (111) surface: (a) the 16c-m site is occupied by Li; (b) the 16c-m and 16c-n sites are occupied by Li. All the energies refer to the Fermi level.

Formation energy

The “formation energy” is the energy needed to form special state. See below for details:

(1) For the first kind of Li-rich surface, that is, the 16c-m site occupied by Li on the surface, the formation energy is defined as:

$$E_{formation} = (E_{LTO(16c)} - E_{LTO(no)} - 2 * E_{Li}) / 2$$

where $E_{LTO(16c)}$, $E_{LTO(no)}$ and E_{Li} are the calculated total energy of the surface system with Li atoms symmetrically occupying the 16c-m sites on the top and the bottom surfaces, the initial model with none of Li atoms occupying the 16c-m sites, and the metallic Li, respectively.

Since the formation energy of one lithium atom occupying the 16c-m site is calculated to be -2.92 eV¹, the 16c site at the outmost surface tends to be occupied with Li⁺ ions.

(2) As for the second and Li-richer configuration (the 16c-m and 16c-n sites occupied by Li), the corresponding formation energy is defined as:

$$E_{formation} = (E_{LTO(16c-16c)} - E_{LTO(16c)} - 2 * E_{Li}) / 2,$$

where $E_{LTO(16c-16c)}$ is the calculated energy when lithium atoms occupy both the 16c-n site and the 16c-m site.

With the 16c-m site occupied with Li, the formation energy of one lithium atom further occupying the 16c-n site is calculated to be -0.97 eV¹. Therefore, the 16c-n site tends to be further occupied with Li for lithium-richer surface if Li source is excess.

Ti³⁺ and Ti⁴⁺ population calculations

The systems of LiTiO₂ (spinel, $Fd\bar{3}m$) and TiO₂ (anatase, $I4_1/AMD$) in bulk phase were studied using a primitive cell. The pseudo-potentials used were Li (2s¹ 2p⁰), O (2s² 2p⁴) and Ti (3d³ 4s¹) with PBE as the exchange-correlation functional. The Hubbard-type U ($U_{eff}=U-J=2.5$ eV, $J=1.0$ eV) calibration was also used for the Ti-3d electrons. All the atoms and cell parameters were relaxed using Γ -centered k -point meshes with spacing about 0.03 Å⁻¹. Denser

k -point meshes with spacing less than 0.02 \AA^{-1} were used for the static calculations and then the Bader charge analysis was conducted to obtain the population of Ti.

The population of Ti is calculated to be 1.76 in LiTiO_2 and 1.33 in TiO_2 . Therefore, the population for the Ti^{3+} and Ti^{4+} is treated as 1.76 and 1.33, respectively.

Li surface

The $\text{Li}(\text{FM}\bar{3}\text{M})$ surfaces were modeled with more than 12 Li layers. The vacuum slab thickness is 40 \AA . The $\text{Li}(1s^1 2p^0)$ pseudo-potential was adopted with PBE as the exchange-correlation functional. All the atoms were relaxed using Γ -centered k -point meshes with spacing less than 0.037 \AA^{-1} . For the static calculations, the spacing of k -point meshes was less than 0.022 \AA^{-1} . Fig. S5 shows the surface models and the corresponding average electrostatic potential energy plots along c direction.

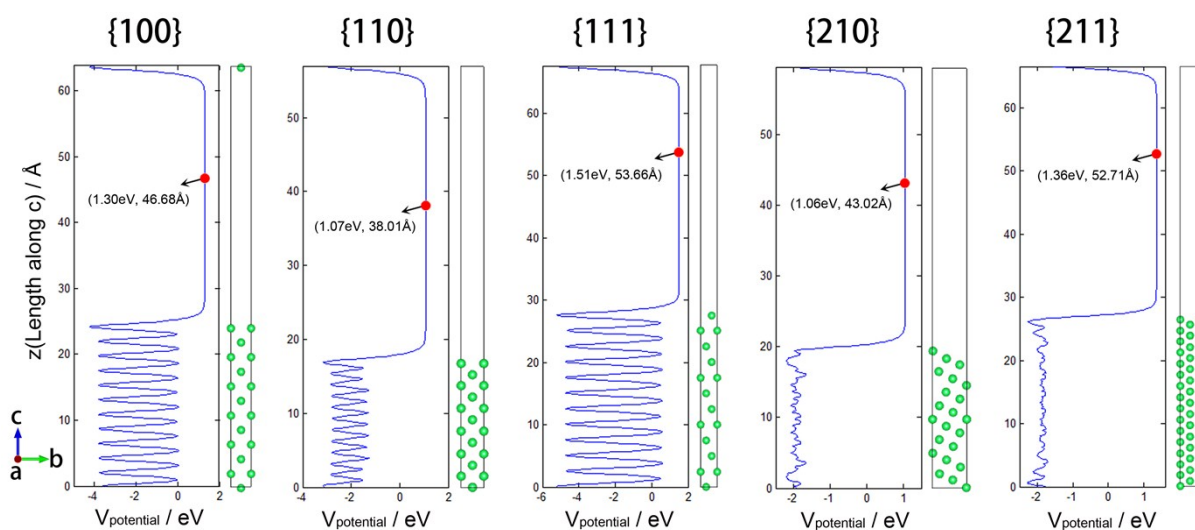


Fig. S5 (a) Models and average electrostatic potential energy plot along c direction of the five low-index surfaces of Li metal ($\text{FM}\bar{3}\text{M}$), $\{100\}$, $\{110\}$, $\{111\}$, $\{210\}$ and $\{211\}$.

According to Fig. S5, the vacuum level is 1.30, 1.07, 1.51, 1.06 and 1.36 eV for Li $\{100\}$, $\{110\}$, $\{111\}$, $\{210\}$ and $\{211\}$ surfaces, respectively. Combining the vacuum level with the calculated Fermi level, we can obtain the workfunction of different indexes of Li surfaces, as listed in Table S2. Therefore, the average surface workfunction of Li metal can be calculated to be 2.76 eV.

Table S2. Calculated vacuum level (ϕ), Fermi level (μ) and workfunction (Φ) of different indexes of Li surfaces.

Index	{100}	{110}	{111}	{210}	{211}
$z_\phi / \text{\AA}$	46.68	38.01	53.66	43.02	52.71
ϕ / eV	1.30	1.07	1.51	1.06	1.36
μ / eV	-1.37	-1.72	-1.41	-1.53	-1.46
Φ / eV	2.67	2.79	2.92	2.59	2.82

Note: z_ϕ is coordinate on the c axis of the selected plane with planar average electrostatic energy as the vacuum level.

Experimental details

The electrode sheet was fabricated by spreading the slurry of the commercial $\text{Li}_4\text{Ti}_5\text{O}_{12}$ powder (Altainano, with a tap density of 0.71 g/cm^3), carbon black and polyvinylidene fluoride (PVDF) dissolved in N-methylpyrrolidone (NMP) at a weight ratio of 8:1:1 onto an aluminum (Al) foil. The electrode sheets were then dried under vacuum at $100 \text{ }^\circ\text{C}$ for 8 h. The half cells were assembled with fresh lithium (Li) foil as the counter electrode, separated by Celgard 2400, and 1 mol L^{-1} LiPF_6 dissolved in the solvent of ethylene carbonate (EC) and dimethyl carbonate (DMC) (1:1 v/v) as the electrolyte in an Ar-filled glove box (MBraun, Lab Master 130). The test cell was galvanostatically cycled between 1.0 and 2.5 V vs. Li^+/Li on a Land BA2100A battery tester (Wuhan, China). The cell is disassembled and the sheet is then washed by DMC solvent for several times and then pumped dry in a vacuum chamber for 10 h. The powder from that sheet is then used for Fourier-transformed infrared (FTIR) test. For the recording of the FTIR spectra, the powder was dispersed in dried KBr, pressed into pellet, and irradiated in the vacuum chamber of a Vertex 70v spectrometer (Bruker Optics, Germany) with a transmission mode at a resolution of 4 cm^{-1} .

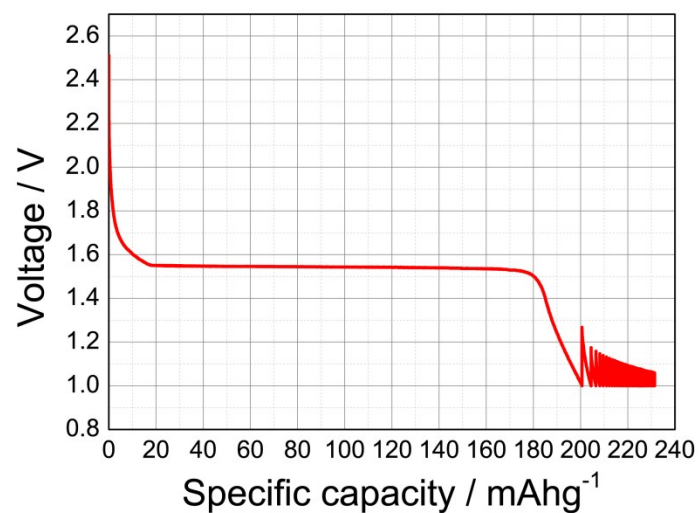


Fig. S6 The quasi “galvanostatic” discharging curve of $\text{Li}_4\text{Ti}_5\text{O}_{12}$.

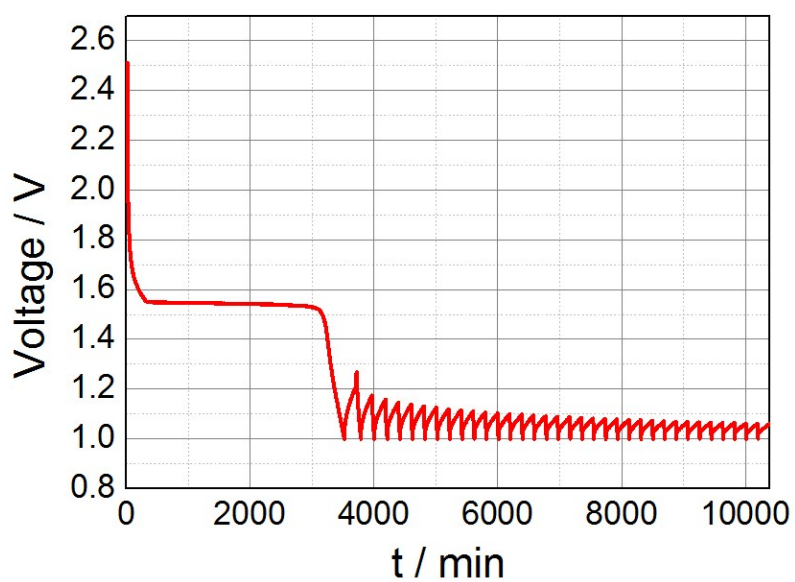


Fig. S7 The quasi “galvanostatic” discharging curve of $\text{Li}_4\text{Ti}_5\text{O}_{12}$ vs. time.

References

1 Y. Gao, Z. Wang and L. Chen, *J. Power Sources*, 2014, **245**, 684.